Spanish Journal of Palaeontology 40 (1), 115–124, 2025
https://doi.org/10.7203/sjp.30611
Sociedad Española de Paleontología ISSN 2255-0550 / eISSN 2660-9568

OPEN ACCESS RESEARCH ARTICLE

Phalangeal formula, topological insights, and symmetry in the manus of Lepidosauria

Fórmula falangeal, abordajes topológicos y simetría en la mano de Lepidosauria

Gabriela FONTANARROSA, Daniel Andrés DOS SANTOS & Diego RASSKIN-GUTMAN

Abstract: The phalangeal formula (PF) describes the skeletal configuration of the digital regions of the autopodia. The plesiomorphic phalangeal formula (PPF) for the Lepidosauria manus is 2-3-4-5-3. Previous research identified 53 unique PFs in lepidosaurians. Here, we propose a new analytical method treating the PF as a matrix, applying image processing techniques to analyze new organizational patterns including symmetry. We quantified the degree of symmetry of the 53 lepidosaurian PFs through a symmetry score capturing the overlap between the original images and their transformed counterparts after specific geometric operations. We found that the PPF revealed a previously unnoticed diagonal axis of symmetry, a pattern highly improbable compared to thousands of randomly generated PFs. In a PCA of the 53 lepidosaurian PFs symmetry scores, PC1 was significantly correlated with the total number of phalanges whereas PC2 reflected the variability in phalangeal counts among different digits. The PCA effectively summarized the underlying variance of the symmetry scores data, elucidating a reduction trend in phalanx count (PC1) and the degree of diversity of PF arrangements (PC2). This approach is useful for addressing symmetry in meristic characters and systems of articulated pieces which could reveal hidden symmetry patterns in other lineages.

Resumen: La fórmula falangeal (FF) describe la configuración esquelética de las regiones digitales del autopodio. Investigaciones previas identificaron 53 fórmulas únicas en las manos de Lepidosuauria siendo 2-3-4-5-3 la fórmula falangeal plesiomorfica (FFP). Aquí proponemos un nuevo método analítico que trata a la FF como una matriz, aplicando técnicas de procesamiento de imágenes para analizar nuevos patrones organizativos, incluida la simetría. Cuantificamos el grado de simetría de las 53 FFs mediante una puntuación de simetría que captura la coincidencia entre las imágenes originales y sus versiones transformadas tras ciertas operaciones geométricas. Descubrimos que la FFP revela un eje de simetría diagonal no advertido anteriormente, un patrón altamente improbable comparado con miles de FFs generadas aleatoriamente. En un análisis de componentes principales (PCA) de los valores de simetría de las 53 PFs, el CP1 mostró una correlación significativa con el número total de falanges, mientras que el CP2 reflejó la variabilidad en la cantidad de falanges entre los distintos dedos. El PCA resumió eficazmente la variabilidad subyacente de los datos, revelando una tendencia de reducción en el número de falanges (CP1) y el grado de diversidad de arreglos de FF (CP2). Este enfoque podría revelar patrones de simetría ocultos en otros linajes.

Received: 1 July 2024
Accepted: 8 november 2024
Published: 24 March 2025

Corresponding author:
Daniel Andrés Dos Santos
dadossantos@csnat.unt.edu.ar

Keywords:
Form organization
Limb evolution
Manus configuration
Digits

Palabras-clave:
Organización de la forma
Evolución de las extremidades
Configuración de la mano
Dígitos

INTRODUCTION

The autopod is the distal end of the characteristic tetrapod limb. It may have originated in the Late Devonian period (385–359 Ma) and it is considered, at least partially, homologous to the sarcopterygian fish fins (Coates, 1994; Shubin *et al.*, 2006; Hall, 2007; Boisvert *et al.*, 2008; Nakamura *et al.*, 2016; Cloutier *et al.*, 2020). The skeleton of the manual autopod is regionalized and includes the carpals, metacarpals, and the series of phalanges that make up each finger (Romer, 1956; Hopson, 1995). The phalangeal formula (**PF**) has been used to characterize phalangeal organization for at least two centuries. This formula is a numerical expression that encodes a manus or foot skeletal configuration by indicating, sequentially from medially to laterally, the number of phalanges of each digit of the manus/pes of a tetrapod taxon (Romer, 1956). There exists a consensus that the Amniota and Lepidosauria manual plesiomorphic phalangeal formula (**PPF**) is 2-3-4-5-3 (Greer, 1991; Fedak & Hall 2004; Fontanarrosa *et al.*, 2021a, 2024a). Thus, considering the number of phalanges per digit, the PPF reflects an ectaxonic condition, with

© The Author(s) 2025. This is an open-access article distributed under the terms of the Creative Commons Attribution 4.0 International License (for details please see http://creativecommons.org/licenses/by/4.0/), which permits use, copy, adaptation, distribution, and reproduction in any medium or format, as long as you give appropriate credit to the original author(s) and the source.

digit IV having the most phalanges. Deviations from this plesiomorphic formula within Amniota include reductions and additions (hyperphalangy), the latter being a rare condition in terrestrial amniotes (Greer, 1992; Shapiro, 2002; Shapiro *et al.*, 2003; Fedak & Hall, 2004; Kohlsdorf & Wagner, 2006; Russell & Bauer, 2008; Fontanarrosa *et al.*, 2021a, 2024a).

In previous work, Fontanarrosa *et al.* (2021a) analyzed the PFs in Lepidosaurian's manus and found a list of 53 unique formulations. This work shows that the set of known PFs comply (to a proportion associated with an extremely low probability of being due to chance) with two properties of phalangeal count per digit, namely the ordering rule (DI ≤ DII ≤ DIII ≤ DIV ≥ DV), and the contiguity relationship (neighbor digits differ on average in one phalanx). These patterns exhibited by the known PFs suggest that, rather than each digit evolving an independent character, they are highly integrated, in line with Klingenberg and Zaklan (2000). Both properties are easily observed in the PPF. Fontanarrosa *et al.* (2024a) demonstrate that the evolutionary trajectories of PFs across Lepidosauria lineages predominantly follow a pattern of evolutionary stasis. Among the 53 known manual PFs within this clade, the PPF exhibits a greater tendency to remain identical across successive phylogenetic tree nodes, *i.e.*, it is inherited without changes in the descendant nodes.

The manual skeletal elements can be described by their organization regarding their main axes (lateromedial and proximodistal). A main pattern shared by the tetrapod lineages is that the autopodial elements are polarized following the proximodistal axis. Moreover, frequently, anatomists have described the tetrapod manus acropodium (*i.e.*, the region containing the phalanges) as bilaterally symmetrical organized about a proximodistal axis traversing digit III, which divides the preaxial and postaxial regions (known as the *mesaxonic condition;* Hopson, 1995; Russell *et al.*, 1997; Russell & Bauer, 2008).

Symmetry implies proportionality within a whole and among its parts, referring to the distribution of equivalent components repeated with regularity in a system (Lederman & Hill, 2004). Morphological symmetry, resulting from the repetition of parts in different orientations, is common in the body plans of most organisms (Savriama & Klingenberg, 2011). It is mathematically defined as the invariance of results obtained by applying a series of *transformation operations* on various systems: material objects, geometric shapes, or abstract entities (*e.g.,* bi-dimensional objects, tri-dimensional objects, mathematical equations, musical chords). Thus, a system is symmetrical if, when such a transformation is applied to it, it results in a system indistinguishable in appearance from the original system (Weyl, 1952; Lederman & Hill, 2004). Transformations include rotation, reflection, and translation of the original geometric shape. According to the transformations applied to the entity, various types of symmetry are obtained: spherical, reflective, cylindrical, translational, anti-translational, and roto-reflective, among others (Weyl, 1952; Martin, 1996). For example, reflective or bilateral symmetry is characterized by the presence of a single plane (or axis if bidimensional), around which a reflection transformation (or flip) produces a final shape identical to the original. A geometric shape with perfect bilateral symmetry implies a distribution concerning a single symmetry plane/axis in which each point of the shape is associated with another point (its *image*), meeting the following conditions: (1) the distance from a point and its corresponding *image* point to the symmetry plane/axis is the same, and (2) the segment that joins a point with its *image* counterpart is perpendicular to the symmetry plane/axis. In natural systems, it is reasonable to expect slight misalignments concerning idealized forms, and in fact, there are approaches for measuring the degree of departure from bilateral symmetry (Zabrodsky *et al.*, 1995; Köhler, 1993) as well as subtleties due to fluctuating asymmetry (Palmer & Strobeck, 1986; Klingenberg, 2015).

Studies of symmetry have traditionally relied on measuring lengths or angles on the left and right sides of organisms. However, with the introduction of geometric morphometrics, Klingenberg *et al.* (2002) provided a mathematical and computational framework for analyzing biological symmetry based on shape. This approach focuses on the geometric configuration of landmarks, ignoring differences due to position or orientation (Klingenberg & McIntyre, 1998; Klingenberg, 2015). While geometric morphometrics offers clear advantages, it is limited to complete structures without movable parts, making it unsuitable for articulated skeletal systems like the autopod, which contains numerous joints and mobile elements (Nebreda *et al.*, 2020).

Here, we propose an approach to mathematically capture the organizational patterns of the acropodium that filters out non-essential information regarding the acropodial configurations related to size, shape, and orientation. The proposal uses the positional information of each phalanx to construct a matrix in which columns represent consecutive digits along the lateromedial axis (abscissa) and rows represent phalangeal positions within the proximodistal axis (ordinates). Each entry or cell of the matrix corresponds to a pixel in the respective image. By doing this, image processing techniques such as symmetry operation transformations can be applied to analyze possible patterns. This work aims to recognize global organizational patterns after geometric image operations involving reflections and rotations. We ask whether some organization pattern is hidden within the structure of the PPF and how the set of PFs observed within the lepidosaurian clade is ordered according to symmetry operations.

METHODS

Data

We used the PFs dataset (Fontanarrosa *et al.*, 2021a, 2024b) of manus configurations of Lepidosauria. This PF data set has been compiled using information from specialized literature and own records from x-rays, CT scans, cleared and stained specimens, and dried osteological specimens. The sample included members of 33 extant families within Squamata of every main clade (Gekkota, Scincoidea, Lacertoidea, Anguinomorpha, Iguania, and Serpentes), the extinct family Aigialosauridae (Anguimorpha), members of the Stem clades of extant representatives (Stem Gekkotan and Stem Serpentes), and members (both extinct and extant) of the squamate sister group Rhynchocephalia (Sphenodontidae).

From phalangeal formula to images

We propose to represent the acropodium as a two-dimensional square matrix using two axes: the lateral dimension for sequential digit arrangement along the x-axis (columns) and the proximodistal axis for sequential phalanx organization within each digit along the y-axis (rows). For similar approaches, see for instance Fontanarrosa *et al.* (2021b) and Fratani *et al.* (2025). This allows us to encode the phalangeal formula into a binary matrix, representing the presence or absence of phalanges in each cell of the matrix (Fig. 1). Each cell in the matrix can have one of two possible states: 1 (indicating the presence of a phalanx) or 0 (indicating the absence of a phalanx). Cells filled are the relevant ones. Finally, we generate an image where pixels represent the cells, with contrasting colors indicating the presence or absence of a phalanx in the pertinent position.

Transformation operations and measurement of symmetry

Matrix transformation operations involve altering the arrangement of elements within the matrix through rotation, reflection, and translation. These transformations produce isomorphic results; *i.e.*, they preserve the neighborhood relationships among homologous pixels and maintain a one-to-one correspondence among all pixels of the matrix (Martin, 1996). The application of transformation operations is a methodological step used in other approaches to study symmetry such as geometric morphometric symmetry analyses (Klingenberg, 2015). Similarly, in this study, we apply a series of predefined rotations and reflections (Martin, 1996) to the original matrix (input). Specifically, we implement a series of three basic types of transformation operations (**TOs**): vertical reflection, horizontal reflection, and 90° clockwise rotation as well as a trivial instance that involves no transformations. We exemplify these actions using the PPF as the input image at the onset of several series of three consecutive symmetry operations (Fig. 2). The outcome derived from the first TO step is used as the input for the next transformation, and so on. Thus, the final output for each series results from the

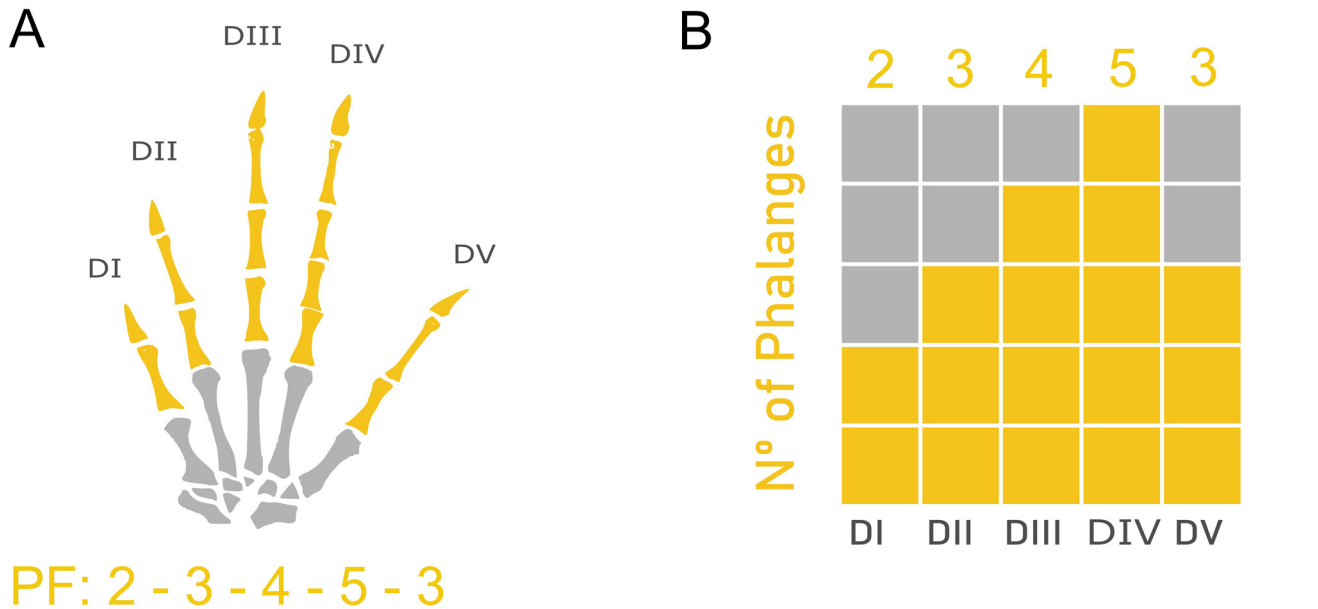

Figure 1. From Phalangeal Formula to Image. **A,** The figure shows a schematic representation of the right autopodium in dorsal view of *Phymaturus* sp. (Squamata: Liolaemidae) depicting the plesiomorphic phalangeal formula for Lepidosauria (2-3-4-5-3). Phalanges are highlighted in yellow; **B,** matricial image derived from the phalangeal formula configuration in A. The X-axis (columns) represents digits I-V. The Y-axis (rows) represents successive phalanges from proximal to distal in each digit. The matrix is binary-filled. Each cell in B is colored yellow if the corresponding element is present in A; otherwise, it is colored gray. This binary matrix image, derived from the phalangeal formula, will serve as our study object in subsequent analyses.

concatenation of TOs steps. Since we carry out three types of TOs, each occurring or not, we end up with 2^3 = 8 final outputs. Each triad of transformations is aimed at testing specific symmetrical properties of the image under study.

As mentioned above, the invariance of an object after a particular transformation applied to it defines its symmetry. The degree of agreement between the original input and final output images was measured to assess the degree of symmetry adjustment across the different series of TOs. For that purpose, we calculated a Symmetry Coefficient (**SC**) based on the recall or sensitivity index in information retrieval (Powers, 2011). In this context recall measures the proportion of relevant cells in the original matrix that are also occupied in the final output matrix. The SC quantifies the similarity between the transformed image and the original, achieving a value of SC = 1 when the images are identical following the symmetry operations.

The different series of TOs are arranged in rows across Figure 2. Each series can be identified by a combination of symbols {H:0, H:1}, {V:0, V:1}, and {R:0, R:1}, denoting the occurrence or absence of horizontal flip, vertical flip, and 90° clockwise rotation, respectively. These combinations allow us to assess the following eight types of possible symmetry operations (see also Figure 2):

1. H:0 V:0 R:0 - Identity operation, no transformations (baseline).
2. H:0 V:0 R:1 - 90° clockwise rotational symmetry.
3. H:0 V:1 R:0 - Reflective symmetry along the proximo-distal axis.

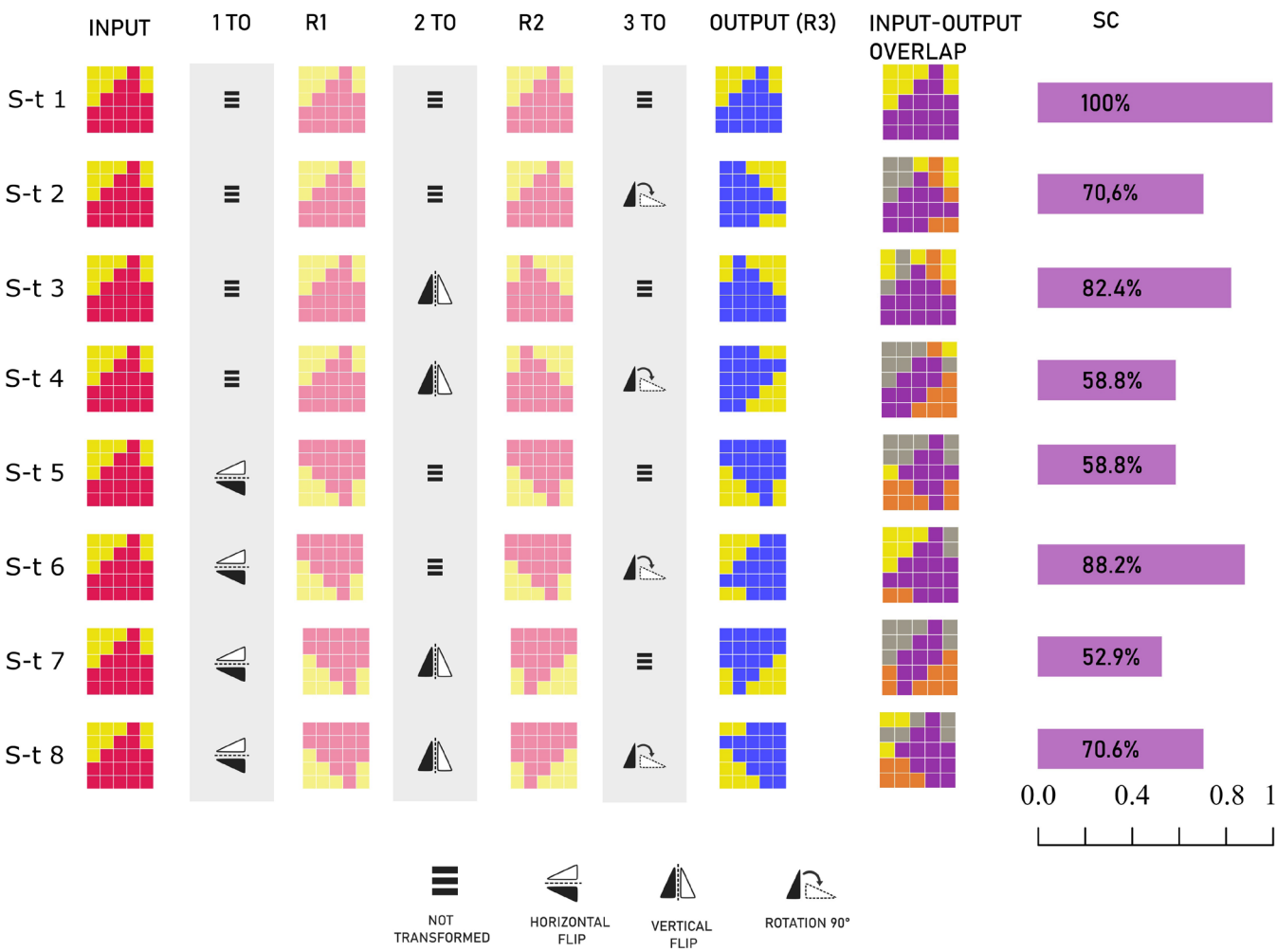

Figure 2. The figure shows the successive transformation operations over the matrix representation of the plesiomorphic phalangeal formula of the lepidosaurian manus through three transformation steps (gray columns 1TO-3TO; each type of transformation is indicated by an icon). Input: Displays the initial matrix representation. All images are identical here, ensuring consistency for comparisons among symmetry operations. After each transformation step, the matrix is updated from the result of the previous transformation. The third result (Output (R3)) is the final output and is exclusive of each symmetry type (S-t 1-8) showing the matrix representation in blue color. Input-Output Overlap: Displays the overlapping of the input and output matrices. Both gray and orange pixels denote discordance, with the orange pixels indicating cells originally marked in the input but lacking correspondence in the output. Symmetry Coefficient (SC): Shows percentage bars of the recall or sensitivity, indicating the pairwise overlap of occupied cells between input and output matrices. It measures the fraction of cells of the input that remain occupied in the output.

4. H:0 V:1 R:1 - Reflective symmetry along the inverse diagonal from SW to NE corner.
5. H:1 V:0 R:0 - Reflective symmetry along the latero-medial axis.
6. H:1 V:0 R:1 (transpose) - Reflective symmetry along the main diagonal from NW to SE corner.
7. H:1 V:1 R:0 - 180° rotational symmetry.
8. H:1 V:1 R:1 - 90° counter-clockwise rotational symmetry.

Analysis of patterns in the phalangeal formula

To explore the PPF organizational properties, we identified the symmetry operation that maximizes SC scores. The transformation resulting in the highest overlap percentage is designated as the leading TO series for this specific plesiomorphic manus configuration. A high SC score associated with this TO series suggests it represents the predominant symmetry type within the image. Statistical significance was assessed by computing SC values for the target symmetry operation across randomized scenarios of PFs. In these scenarios, phalangeal formulae (PFs) were generated by randomly sampling counts from a truncated Poisson distribution (Plackett, 1953; Singh, 1978) with a mean (lambda) of 3.4, which matches the mean phalangeal count observed in the PPF. The distribution was constrained between 0 and 5 to reflect the typical variation in most lepidosaurian species (Fontanarrosa *et al.*, 2021), thus providing a realistic, statistically sound, and manageable framework for generating the null model.

We also examined the symmetry profiles across the comprehensive dataset of observed PFs compiled by Fontanarrosa *et al.* (2021a, 2024a, 2024b). We computed SC values for various transformation operations, excluding the trivial series with no transformations. Each type of symmetry explored corresponds to an analytical variable. Subsequently, a Principal Component Analysis (**PCA**) was applied to this multivariate dataset, reducing its dimensionality by summarizing the variance across the symmetry variables. This projection into a reduced dimensional space allows for the study of general patterns and typologies of PFs based on their positions within the factor map. All analyses and visualizations were performed using the R software (R Core Team, 2023; version 4.2.2), leveraging packages such as ade4 (version 1.7-20) and extraDistr (1.10.0).

RESULTS

Implementing the three-step transformation operations series on the PPF configuration generates eight different output matrices (Fig. 2). Excluding the trivial case of no transformations, the sixth action (H:1 V:0 R:1 = vertical flip followed by a 90° clockwise rotation) yields the highest degree of symmetry (~88%), as measured by the recall rate of relevant instances in the input (red cells) retrieved in the output (blue cells). This action is equivalent to the transposition of the original matrix and corresponds to assessing symmetry along the main diagonal running from the NW to the SE corner of the image (considering the right manus in the dorsal view). The second-highest symmetry score corresponds to the reflective symmetry along the proximodistal axis (82.4%).

Singularity of the plesiomorphic phalangeal formula as indicated by a symmetry operation

Upon conducting the null generation of 10,000 phalangeal formulae with counts drawn from a truncated Poisson distribution, we obtained a left-skewed distribution for the Symmetry Coefficient (SC; mean = 0.626, SD = 0.168, median = 0.647) associated with the sixth operation for assessing symmetry along the main diagonal (Fig. 3). Notably, the empirical SC value calculated for the PPF (~88%) falls in the rejection area at the 5% significance level on the right tail. Therefore, we can confidently reject the null hypothesis that suggests no organizational pattern of phalangeal counting across digits.

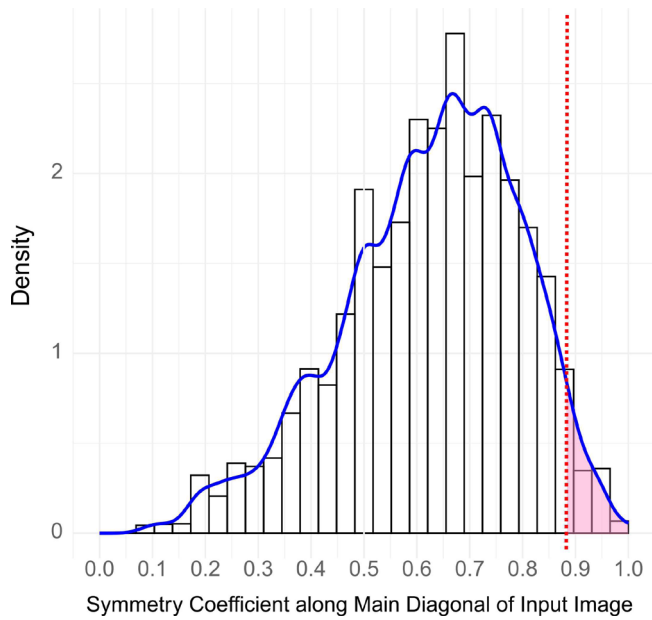

Figure 3. Distribution of the Symmetry Coefficient (SC) under randomized scenarios (null generative model of phalangeal formulae involving 10,000 repetitions). Each phalangeal formula is translated into a binary square matrix and then into an image. Here, the SC estimates the degree of overlap between input and output images after mirroring along the main diagonal from the NW to SE corner in each squared image. SC measures the fraction of occupied cells that have been retrieved after this transformation over the total amount of occupied cells in the input. The red dotted line indicates the observed SC value. The probability of observing an SC as extreme as or more extreme than the observed value is less than 0.05.

Ordination of the empirical set of phalangeal formulae

A Principal Component Analysis (PCA) was performed on a dataset comprising the unique phalangeal formulae known from lepidosaurian species and the calculated coefficients of the symmetry operations. The input data submitted to PCA consisted of 53 rows and 7 columns (symmetry scores derived from TOs series), excluding the trivial transformation operation. Thus, each point data corresponds to a single phalangeal formula. The very first two components (*i.e.*, Axes 1 and 2) accounted for a substantial amount (= 88.45%) of the total variance held by the data (Fig. 4A). Except for the 3rd TO regarding vertical flipping (for assessing a mirror condition across the manus proximo-distal axis), the remaining operations load heavily on the Axis 1 (Fig. 4B). Overall patterns of change can be recognized throughout the scatter diagram of the PCA. Reduction in the number of phalanges proceeds from left to right in the factor map (Fig. 3C), while homogenization or equalization occurs from bottom to top (Fig. 4D).

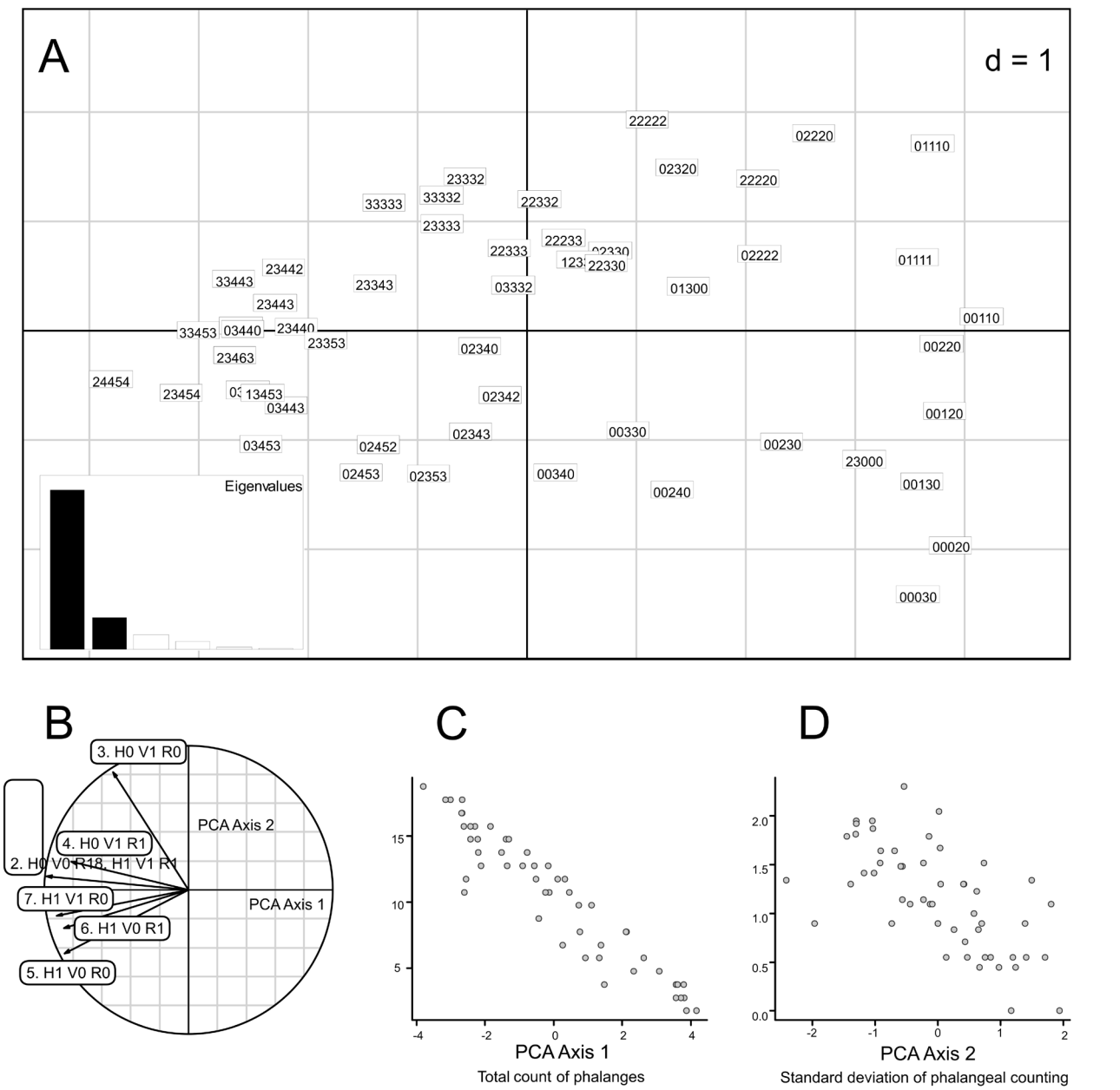

Figure 4. Principal Component Analysis (PCA) for variables underlying the transformation operations of the input image for the lepidosaurian dataset. **A,** Scatter Plot of the set of phalangeal formulae projected on the first two axes of PCA. Inlet: bar plot for eigenvalues; **B,** correlation circle. It shows the relationships between all variables of the symmetry operations. Positively correlated variables are grouped. The distance between variables and the origin measures the quality of the variables on the factor map. The closer a variable is to the circle of correlations, the better its representation on the factor map; **C,** relationship between the total count of phalanges and the scores of point data along PCA Axis 1. The overall trend shows a reduction from left to right; **D,** relationship between the dispersion of phalangeal counts and the scores of point data along PCA Axis 2. Homogenization occurs from bottom to top.

DISCUSSION

Comparative analysis of morphological features is helped by the use of a mathematical abstraction. Quantifying anatomical parts can be considered as the construction of a model that represents such parts, a process of abstraction that highlights some features while disregarding others. This applies to the phalangeal formula, a simple integer sequence (a unidimensional vector representing the number of phalanges in each digit of the manus or pes). PF represents a model that has yielded important information about the evolution of many tetrapod lineages, including lepidosaurians (Richardson & Chipman, 2003; Shapiro *et al.*, 2007; Russell & Bauer, 2008; Fontanarrosa *et al.*, 2021a, 2024a). Phalangeal evolution can be effectively examined through various mathematical approaches. For instance, Nebreda *et al.* (2020) tackled digital evolution by representing phalangeal variation in the Maniraptoran manus as an X-Y coordinate matrix and utilizing Euclidean distances.

The organization of the manus reverberates in the information encoded in a phalangeal formula. As already mentioned before, previous work has found that lepidosaurians have a repertoire of 53 unique formulations and two properties: an ordering rule and a contiguity relationship (Fontanarrosa *et al.*, 2021a), which are very apparent in the 2-3-4-5-3 plesiomorphic condition. Even though the number of phalanges could indicate adaptation to a specific ecological niche, the analysis in Fontanarrosa *et al.* (2021a), showed that the PF tends to show, instead, a phylogenetic constraint (*i.e.,* the exploration of the phylogenetic tree reveals that lineages often share the phalangeal configuration of their ancestral node). In the present work, we have expanded the representation of the PF to generate a matrix model; each formula is represented as an image of pixels that can be manipulated using simple invariant transformations to find more complex organizational symmetry patterns embedded in each one of them. Two main results were obtained by transforming and further analyzing this model: (1) the plesiomorphic manus of lepidosaurians (the same formula for the plesiomorphic amniote condition) exhibits a strong fit to a diagonal axis of symmetry, and (2) the reduced symmetry space of phalangeal formulae in lepidosaurians is ordered along two main factors that can be interpreted as surrogates of eco-evo-devo signals.

Symmetry

The evolution of morphological symmetry is of interest in and of itself (Klingenberg, 2015). In multicellular organisms, symmetry is an instance of how meristic, repeated characters are organized (Rasskin-Gutman, 2003). For example, in the tetrapod skeleton, the repetition of carpal elements in the manus can generate symmetrical arrangements. When this arrangement is the same around the axis provided by the digit III, a symmetry known as “mesaxonic” occurs; whereas other “ectaxonic” imply a predominant development in some morphological attribute such as length, width or phalangeal number. This difference can be functionally significant in some cases, although some studies have reported that both conditions can carry out similar functions; for example, in primates (Lemelin & Schmitt, 1998). Although there are no specific studies on the bilateral symmetry of anatomical parts within manus (that is, particular to each manus), several authors recognize the presence of a pattern of bilaterality in some tetrapod lineages. Hopson (1995) reported a higher degree of symmetry in the manus of therapsids compared to other synapsids and interpreted this pattern as a morpho-functional advantage for the particular parasagittal body posture of that clade.

There has been an extensive development of methodologies to measure radial and bilateral symmetry in living organisms based on various techniques, with geometric morphometrics being the most developed. These methodologies have greatly contributed to the theoretical framework related to embryonic development, environmental stress, and hybridization and or fitness (Savriama & Klingenberg, 2011). However, when attempting to address an articulated skeletal system, geometric morphometrics encounter difficulties. Our approach, unlike geometric morphometrics, disregards shape and focuses on topology and meristic series.

Our results have found a new kind of symmetry in the ectaxonic condition of the plesiomorphic manus. Indeed, after performing a series of rotational composite transformation operations, the highest symmetry score for the plesiomorphic condition corresponded to the combination of vertical flip and 90º clockwise rotation. This particular combination of these two basic transformations is equivalent to a single reflection transformation operation over a diagonal axis crossing the autopodium from proximo/lateral to distal/medial. We further supported this finding by performing an analysis of 10,000 randomly generated phalangeal formulas, confirming that this diagonal axis of symmetry is not common. This strongly suggests that the ectaxonic plesiomorphic phalangeal formula has a preferred symmetry that is diagonal. How can we interpret this symmetry pattern? As the patterns of topological relationships of each phalanx in a given phalangeal formula can be reminiscent of local self-organizational processes during embryonic development (Raspopovic *et al.*, 2014; Fontanarrosa *et al.*, 2021a; Hentschel *et al.*, 2024), an explanation for this new finding could be based on the morphogenetic processes that form the manus. The interplay between the growth axes of the limb bud (proximodistal and lateromedial) could explain the identified diagonal symmetry. This pattern may reflect an underlying organization in limb development, where the two growing axes influence the final distribution of phalanges in the digits. Moreover, it has been noted that the digital arc begins to form posteriorly and turns anteriorly across the distal mesenchyme (Shubin &

Alberch, 1986; Gilbert, 2000). This "diagonalization" that occurs during development can be translated into the final pattern of the adult manus, as shown by our results.

The above-mentioned interplay leads us to consider that the two conceptual domains of symmetry in biology intermingle here, namely symmetry as a pattern and symmetry as a process (Palmer, 1994; Rasskin-Gutman, 2003). The former encompasses the morphological expression of symmetrical traits in organisms, which emerge as a property of multicellular life. The latter refers to the conditions, whether symmetrical or not, that shape the form of embryos and adults. Further studies may evaluate the evolutionary and developmental relevance of the diagonal axis found in our results.

Dimensions of a Symmetry Space

An empirical morphospace can highlight interesting patterns within a large phylogenetic group. By studying how forms occupy a morphospace in discrete areas, we can infer the existence of internal constraints that prevent an even distribution (Fontanarrosa *et al.*, 2021a). Our principal component analysis of the seven non-trivial symmetry variables delivered an ordering of the 53 unique phalangeal formula configurations of Lepidosauria along the first two components, which accounted for 88.4% of the variance. Thus, we generated an empirical symmetry space in which PC1 suggested a trend of phalanx reduction, possibly reflecting a phylogenetic signal, while PC2 differentiated PFs into homogeneous (forms with similar or identical phalangeal counts across digits such as 2-2-2-2-2) and heterogeneous groups (forms with more dissimilar phalangeal counts across digits such as 0-0-2-4-0), which could be considered as carrying an adaptive signal. This result reinforces the existence of general trends of bone number reduction across reptilian limbs, a phenomenon underscoring a fundamental principle of morphological evolution observed in various tetrapod lineages (Hall, 2007; Shapiro *et al.*, 2007) as well as with studies suggesting that the autopod form is subject to a cascade of related phenomena, including ecological diversity and locomotory patterns (Delfino *et al.*, 2010). The scatter plot further suggests that lepidosaurians with a higher number of phalanges seem to diverge along the phylogenetic axis into two groups: while both of them reduce their number of phalanges, one is a homogenous group (Fig. 4A, upper-right quadrant) and the other a heterogeneous group (Fig. 4A, lower-right quadrant).

CONCLUSION

To conclude, we have shown that the information encoded in the phalangeal formula can be expanded from a unidimensional vector to a richer 5 × 5 matrix. This analysis unveils the inherent structural properties of the image, offering insights into its organizational characteristics. This model has allowed us to perform image analysis operations that have shown the existence of a neglected diagonal axis of symmetry in the plesiomorphic phalangeal formula, maybe obscured by shape, size, and a wide range of interdigit angles. In addition, we have shown that in the morphospace of symmetry operations, all lepidosaurian formulae can be sorted in order of decreasing number of phalanges that have evolved purportedly into two distinct groups of homogeneous *versus* heterogeneous forms. Several questions arise that should be addressed in the future; for example, are there equivalent phalanges from one side to the other of the diagonal axis of symmetry? Is the equivalence based on development or do they carry some functional significance? To date, there are no well-documented homologies between phalanges, but it could be conceived that different phalanges have equivalent functions in different fingers. Future work using this representation model and other forms of image filtering analysis could lead us to study symmetry patterns that remain hidden from other form abstractions.

Supplementary information. This article has no additional data.

Author contributions. GF conceived the study. DADS led the data analysis. All authors contributed to the discussion of the results and the writing of the manuscript.

Competing interests. The authors declare no conflict of interests.

Funding. Proyecto de Salto Institucional PICT-2021-CAT-II-00058.

Author details. **Gabriela Fontanarrosa**[1], **Daniel Andrés Dos Santos**[2], & **Diego Rasskin-Gutman**[3]. [1]Instituto de Biodiversidad Neotropical (IBN, CONICET-UNT), Consejo Nacional de Investigaciones Científicas y Técnicas (CONICET), Facultad de Ciencias Naturales e Instituto Miguel Lillo, Universidad Nacional de Tucumán (UNT), Yerba Buena, Tucumán, Argentina; gab.fontanarrosa@gmail.com; [2]Cátedra de Bioestadística, Facultad de Ciencias Naturales e Instituto Miguel Lillo, Universidad Nacional de Tucumán (UNT), Miguel Lillo 205, San Miguel de Tucumán, Tucumán, Argentina; dadossantos@csnat.unt.edu.ar; [3]Grupo de Investigación de Biología Teórica, Instituto Cavanilles de Biodiversidad y Biología Evolutiva, Universidad de Valencia, Valencia, España; diego.rasskin@uv.es

Acknowledgements. We would like to express our sincere gratitude to the "PICT Salto Institucional-CONICET" project awarded to Carolina Nieto, with which Gabriela Fontanarrosa (GF) and Daniel A. Dos Santos (DADS) are affiliated as beneficiaries. We also thank Carolina Nieto for her efforts in managing the grant. GF and DADS express their gratitude to the Argentine public education and scientific systems. GF is grateful to Virginia Abdala for her constant support and assistance in refining ideas related to Object Symmetry in the manus. We thank the two anonymous referees for their interesting and constructive comments. DRG thanks the ICBIBE for continuous support, and Miquel De Renzi for almost twenty years of comradery involving art, poetry, culinary experiences, and, of course, some science.

REFERENCES

Boisvert, C. A., Mark-Kurik, E., & Ahlberg, P. E. (2008). The pectoral fin of *Panderichthys* and the origin of digits. *Nature*, *456*, 636–638. doi: 10.1038/nature07339

Cloutier, R., Clement, A. M., Lee, M. S. Y., Noël, R., Béchard, I., Roy, V., & Long, J. A. (2020). Elpistostege and the origin of the vertebrate hand. *Nature*, *579*, 549–554. doi: 10.1038/s41586-020-2100-8

Coates, M. I. (1994). The origin of vertebrate limbs. *Development*, *1994*(Supplement), 169–180. doi: 10.1242/dev.1994.Supplement.169

Delfino, M., Fritz, U., & Sánchez-Villagra, M. R. (2010). Evolutionary and developmental aspects of phalangeal formula variation in pig-nose and soft-shelled turtles (Carettochelyidae and Trionychidae). *Organisms Diversity & Evolution, 10*, 69–79. doi: 10.5167/uzh-43157

Fedak, T. J., & Hall, B. K. 2004. Perspectives on hyperphalangy: Patterns and processes. *Journal of Anatomy*, *204*(3), 151–163, doi: 10.1111/j.0021-8782.2004.00278.x

Fontanarrosa, G., Abdala, V., & Dos Santos, D. A. (2021a). Morphospace analysis leads to an evo-devo model of digit patterning. *Journal of Experimental Zoology Part B: Molecular and Developmental Evolution, 336*, 341–351. doi: 10.1002/jez.b.23026

Fontanarrosa, G., Fratani, J., Vera, M. C., Abdala, V., & Russell, A. (2021b). Perspectives on the repeated evolution of paraphalanges through the lens of theoretical biology. In *Proceedings of the I Congreso Latinoamericano de Evolución (CLEVOL)*.

Fontanarrosa, G., Abdala, V., & Dos Santos, D. A. (2024a). Modeling evolutionary tempo and mode using formal morphological spaces and Markov chain principles. *Journal of Evolutionary Biology, 37*, 76–88. doi: 10.1093/jeb/voad007

Fontanarrosa, G., Abdala, V., & Dos Santos, D. A. (2024b). Phalangeal formula of Lepidosauria [Dataset]. Dryad. doi: 10.5061/dryad.vhhmgqp19

Fratani, J., Fontanarrosa, G., Duport-Bru, A. S., & Russell, A. (2025). Exploring the influence of neomorphic Gekkotan paraphalanges on limb modularity and integration. *Journal of Experimental Zoology Part B: Molecular and Developmental Evolution*, *344*, 14–28, doi: 10.1002/jez.b.23275

Gilbert, S. F. (2000). Developmental Biology. 6th edition. Sunderland (MA): Sinauer Associates. Generating the proximal-distal axis of the limb. Available from: https://www.ncbi.nlm.nih.gov/books/NBK10102/

Greer, A. E. (1991). Limb reduction in Squamates: Identification of the lineages and discussion of the trends. *Journal of Herpetology, 25*(2), 166–73. doi: 10.2307/1564644

Greer, A. E. (1992). Hyperphalangy in squamates: insight on the reacquisition of primitive character states in limb-reduced lineages. *Journal of Herpetology, 26*, 327–329. doi: 10.2307/1564889

Hall, B. K. (2007). *Fins into limbs: Evolution, development, and transformation*. The University of Chicago Press.

Hentschel, H. G., Glimm, T., Glazier, J. A., & Newman, S. A. (2004). Dynamical mechanisms for skeletal pattern formation in the vertebrate limb. *Proceedings of the Royal Society B: Biological Sciences, 271*, 1713–1722. doi: 10.1098/rspb.2004.2772

Hopson, J. A. (1995). Patterns of evolution in the manus and pes of non-mammalian therapsids. *Journal of Vertebrate Paleontology, 15*, 615–39. doi: 10.1080/02724634.1995.10011252

Köhler, A. E. (1993). A second approach to fuzzy symmetries: Fuzzy symmetry requirements. *Computers Mathematical Applications, 25*(1), 17–34. doi: 10.1016/0898-1221(93)90208-D

Klingenberg, P. C. (2015). Analyzing fluctuating asymmetry with geometric morphometrics: Concepts, methods, and applications. *Symmetry, 7*(2), 843–934, doi: 10.3390/sym7020843

Klingenberg, C. P., Barluenga, M., & Meyer, A. (2002). Shape analysis of symmetric structures: Quantifying variation among individuals and asymmetry. *Evolution*, *56*, 1909–1920.

Klingenberg, C. P., & McIntyre, G. S. (1998). Geometric morphometrics of developmental instability: Analyzing patterns of fluctuating asymmetry with Procrustes methods. *Evolution*, *52*(5), 1363–1375. doi: 10.1111/j.1558-5646.1998.tb02018.x

Klingenberg, C. P., & Zaklan, S. D. (2000). Morphological integration between developmental compartments in the Drosophila wing. *Evolution*, *54*(4), 1273–1285. doi: 10.1111/j.0014-3820.2000.tb00560.x

Kohlsdorf, T., & Wagner, G. P. (2006). Evidence for the reversibility of digit loss: a phylogenetic study of limb evolution in *Bachia* (Gymnophthalmidae: Squamata). *Evolution, 60*(9), 1896–1912. doi: 10.1554/06-056.1

Lederman, L. M., & Hill, C. T. (2004). *Symmetry and the beautiful Universe*. Prometheus Books.

Lemelin, P., & Schmitt, D. (1998). The relation between hand morphology and quadrupedalism in primates. *American Journal of Physical Anthropology, 105*(2), 185–197. doi: 10.1002/(SICI)1096-8644(199802)105:2<185::AID-AJPA6>3.0.CO;2-U

Martin, G. E. (1996). *Transformation geometry: An introduction to symmetry*. Springer-Verlag.

Nakamura, T., Gehrke, A. R., Lemberg, J., Szymaszek, J., & Shubin, N. H. (2016). Digits and fin rays share common developmental histories. *Nature*, *537*(7619), 225–228. doi: 10.1038/nature19322

Nebreda, S. M., Navalón, G., Menéndez, I., Sigurdsen, T., Chiappe, L. M., & Marugán-Lobón, J. (2020). Disparity and macroevolutionary transformation of the maniraptoran manus. *Bulletin of the American Museum of Natural History*, *440*, 183–203.

Palmer, A. R. (1994). Fluctuating asymmetry analyses: A primer. In: T. A. Markow (Ed.), *Developmental instability: Its origins and evolutionary implications* (pp. 335–364). Kluwer.

Palmer, A. R., & Strobeck, C. (1986). Fluctuating asymmetry: measurement, analysis, patterns. *Annual Review of Ecology and Systematics*, *17*, 391–421. doi: 10.1146/annurev.es.17.110186.002135

Plackett, R. L. (1953). The truncated Poisson distribution. *Biometrics, 9*(4), 485–488.

Powers, D. (2011). Evaluation: From precision, recall and F-Measure to ROC, informedness, markedness & correlation. *Journal of Machine Learning Technologies, 2*, 37–63. doi: 10.48550/arXiv.2010.16061

R Core Team. (2023). R: A language and environment for statistical computing. R Foundation for Statistical Computing. https://www.r-project.org/

Rasskin-Gutman, D. (2003). Organized mayhem in Bilateria Baupläne: Symmetry and animal complexity. *Coloquios de Paleontología*, *Ext. 1*, 559–567.

Raspopovic, J., Marcon, L., Russo, L., & Sharpe, J. (2014). Digit patterning is controlled by a Bmp-Sox9-Wnt Turing

network modulated by morphogen gradients. *Science*, *345*, 566–571. doi: 10.1126/science.1252960

Richardson, M. K., & Chipman, A. D. (2003). Developmental constraints in a comparative framework: a test case using variations in phalanx number during amniote evolution. *Journal of Experimental Zoology Part B. Molecular and Developmental Evolution*, *296*, 8–22. doi: 10.1002/jez.b.13

Romer, A. S. (1956). *Osteology of the Reptiles*. University of Chicago Press.

Russell, A. P., Bauer, A. M., & Laroiya, R. (1997). Morphological correlates of the secondarily symmetrical pes of gekkotan lizards. *Journal of Zoology*, *241*, 767–790. doi: 10.1111/j.1469-7998.1997.tb05747.x

Russell, A. P., & Bauer, A. M. (2008). The appendicular locomotor apparatus of Sphenodon and normal-limbed Squamates. In: C. Gans, A. S. Gaunt, & K. Adler (Eds.), *Biology of the Reptilia, Volume 21, Morphology I, The skull and appendicular locomotor apparatus of Lepidosauria* (pp. 1–466). Society for the Study of Amphibians and Reptiles, Academic Press.

Savriama, Y., & Klingenberg, C. (2011). Beyond bilateral symmetry: Geometric morphometric methods for any type of symmetry. *BMC Evolutionary Biology*, *11*, 280. doi: 10.1186/1471-2148-11-280

Shapiro, M. D. (2002). Developmental morphology of limb reduction in *Hemiergis* (Squamata: Scincidae): Chondrogenesis, osteogenesis, and heterochrony. *Journal of Morphology*, *254*, 211–231. doi: 10.1002/jmor.10027

Shapiro, M. D., Hanken, J., & Rosenthal, N. (2003). Developmental Basis of Evolutionary Digit Loss in the Australian Lizard Hemiergis. *Journal of Experimental Zoology Part B: Molecular and Developmental Evolution*, *297*, 48–56. doi: 10.1002/jez.b.19

Shapiro, M., Shubin, N., & Downs, J. P. (2007). Limb reduction and diversity in reptilian evolution. In: B. K. Hall (Ed.), *Fins into limbs: Evolution, development, and transformation* (pp. 225–244). The University of Chicago Press.

Shubin, N. H., Daeschler, E. B., & Jenkins, F. A., Jr. (2006). The pectoral fin of *Tiktaalik roseae* and the origin of the tetrapod limb. *Nature*, *440*, 764–771. doi: 10.1038/nature04637

Shubin, N. H., & Alberch, P. (1986). A morphogenetic approach to the origin and basic organization of the tetrapod limb. *Evolutionary Biology*, *20*, 319–387. doi: 10.1007/978-1-4615-6983-1_6

Weyl, H. (1952). *Symmetry*. Princeton University Press.

Singh, J. (1978). A characterization of positive Poisson distribution and its application. *SIAM Journal of Applied Mathematics, 34*, 545–54. doi: 10.1137/0134043

Zabrodsky, H., Peleg, S., & Avnir, D. (1995). Symmetry as a continuous feature. *Transactions on Pattern Analysis and Machine Intelligence, 17*, 1154–1166. doi: 10.1109/34.476508.